

First Principle Study on the Structural Optimization and Electronic Properties of Methylammonium Bismuth Bromide and Methylammonium Gallium Bromide

S. G. Abdu^{a,*}, A. Shuaibu^a, M. Aboh^a, M. S. Abubakar^a

^aDepartment of Physics, Faculty of Science, Kaduna State University, P.M.B. 2339, Kaduna State, Nigeria

Abstract

Ab initio calculations for the structural optimization, and Band Structure analyses of $\text{CH}_3\text{NH}_3\text{BiBr}_3$ and $\text{CH}_3\text{NH}_3\text{GaBr}_3$ (having 8.33% dopant replacement percentage each) as possible replacements for the Lead based perovskite $\text{CH}_3\text{NH}_3\text{PbBr}_3$ were done in this work using Perdew–Burke–Ernzerhof functional of Density Functional Theory as implemented by FHI-aims Code. Molecular visualizations and crystal structures were rendered using JMOL. Optimized lattice constants were calculated for $\text{CH}_3\text{NH}_3\text{BiBr}_3$ and $\text{CH}_3\text{NH}_3\text{GaBr}_3$ to be 9.10 Å and 8.27 Å respectively, and The Lowest Unoccupied Molecular Orbital (LUMO), Highest Occupied Molecular Orbital (HOMO) and calculated band gap, Band Structure and Density of States (DOS) plots were made to analyse the band structures of these crystals and they were found to be metallic with a band gap of 0.00018636 eV and 0.00022286 eV for $\text{CH}_3\text{NH}_3\text{BiBr}_3$ and $\text{CH}_3\text{NH}_3\text{GaBr}_3$ respectively.

Keywords: Band Structure, $\text{CH}_3\text{NH}_3\text{BiBr}_3$, $\text{CH}_3\text{NH}_3\text{GaBr}_3$, DFT, DOS, FHI-aims, Lattice Constant, Optimization, Relaxation

Article History :

Received 17 February 2019

Received in revised form 27 November 2019

Accepted for publication 6 December 2019

Published 31 December 2019

©2019 Physics Memoir. All rights reserved.

1. Introduction

Since the dawn of the 20th century, the evolution of science to find alternate sources of energy has exponentially progressed. From Moore's law regarding technological advancements, this is not so surprising. The search for renewable energy has left scientific minds considering Solar and Wind as the most promising avenues for sustainable, and renewable clean energy [1]. Solar energy is mostly considered because of its availability and capacity to provide constant energy and very little running and maintenance costs. At the forefront of the solar energy front for renewable energy is the use of Methylammonium Lead Halide perovskites (a Perovskite is a solid that has the same cubic crystal

*Corresponding author

Email address: sgabdu@kasu.edu.ng (S. G. Abdu)

arrangement as calcium titanium oxide CaTiO_3 (Clean Energy Institute, 2019)), among other Nano-materials, for the production of solar modules because of their high efficiency in light absorption and applications in photovoltaics [2].

Methylammonium Lead bromide perovskite solar cells have high efficiency and have advanced more rapidly than any other dye sensitized solar cell (DSSC) to date, in a few years since their discovery [1]. Their outstanding performance inspired researches for using them in optoelectronics, such as LED (light-emitting diode), photodetectors and lasers. As much as Methylammonium Lead bromide perovskites show impressive properties for photovoltaic use, their manufacture cost is relatively low and they are relatively easy to manufacture [3]. They are strong candidates for the future of photovoltaics with only disadvantage being that they degrade easily due to environmental factors like temperature and humidity, not making them viable for commercial use.

Lead is a well-known toxic material and its use is being gradually phased out of many applications. Lead is toxic and accumulates in soft tissue and bones, it acts as a neurotoxin that damages nerves and interferes with organic enzymes and their functions. It is worse especially in children: even after treatment, neurological conditions like brain injury and behavioural complications may still result. Because of this toxicity, the application of Lead in the production of various materials that will eventually come in contact with man or nature, has been drastically reduced and the use of Lead in a lot of compounds have been phased out [4].

This research looks to find a viable substitute(s) for Lead in Lead-based perovskites. Considering its position on the periodic table and its physical, electronic, and atomic characteristics, Lead has just a handful of replacements on first glance. It is a post-transition metal thus it has 11 other metals that should replace it. Looking at Lead's atomic number (82), its neighbouring elements Thallium (Tl) and Bismuth (Bi), should be considered viable substitutes because their atomic numbers are close to that of Lead, and they share similar properties.

From looking at the periodic table, it can be seen that Thallium (Atomic Number 81) should be a good theoretical substitute for Lead in the synthesis of perovskites, but it comes at a risk. The same risk posed by Lead. Thallium is also toxic [5]. Nearly tasteless and toxic, soluble Thallium salts were used for making rat poisons and insecticides. They are restricted or banned in a lot of countries, because their indiscriminately harmful. Hair loss is caused by Thallium poisoning even though it may not always show this way. It is historically popular as a weapon for murder, and thallium has gained notoriety as "the poisoner's poison" and "inheritance powder" [6].

Bismuth, on the other hand, is virtually non-toxic unlike its heavy-metal counterparts like Lead and Thallium. It is widely and commonly used in the production of cosmetic powders and certain pharmaceuticals, bismuth subsalicylate, even used to treat diarrhoea. Thus, Bismuth is considered for the compounds $\text{CH}_3\text{NH}_3\text{PbBr}_3$ (Methylammonium Lead bromide) and $\text{CH}_3\text{NH}_3\text{PbI}_3$ (Methylammonium Lead iodide), the suitable replacement for Lead. (Methylammonium Lead bromide) and $\text{CH}_3\text{NH}_3\text{PbI}_3$ (Methylammonium Lead iodide), the suitable replacement for Lead.

On the other hand, Gallium (Ga) (Atomic Number 31) is also a post-transitional metal like Lead but unlike Lead, it is non-toxic like Bismuth. Looking at the results published by Abdulsalam and Babaji [3], Lead was replaced with Germanium (a metalloid with atomic number 32). Gallium may be a better replacement for Germanium because is a post-transitional metal like Lead. Gallium is considered in this case because of its similarity in size to Germanium in an attempt to see if the final results calculated would give better physical properties.

2. Materials and Methods

2.1. Relaxation

In order to calculate the Band Structure and Optical Properties of any material or compound, an optimized system is recommended. Structural optimization involves tweaking the parameters (lattice vectors and atomic coordinates) that digitally represents a compound such that these sets of parameters produce a structure that gives the lowest possible total energy in a simple energy calculation. This is the most stable form of the compound or material. This research was made using Fritz Haber Institute ab initio molecular simulation (FHI-aims) code to calculate the energies for the structural optimization of MABiBr_3 and MAGaBr_3 molecules, using additional software like GRACE (Graphing Advanced Computation and Exploration of data) and JMOL (Java Molecule) to graphically represent data and visualise the molecular structure(s) respectively. In order to do this, first the stable molecular structures of the compounds in question have to be determined. FHI-aims supports these major forms of relaxation algorithms; The various forms of the Broyden-Fletcher-Goldfarb-Shanno (BFGS) algorithm, Fast Inertial Relaxation Engine (FIRE), Conjugate-Gradient (CG) algorithm, and Trust Radius (TRM) algorithm [7]. Trust Radius (TRM) algorithm was used

for this particular compound since it is organic and because TRM is a variation of BFGS that is considerably accurate and less computationally expensive. In the process of relaxation, the atomic coordinates that make up the molecular geometry of the compound are altered and reduced to a point where the total energy of the molecule is at its lowest. This is the most stable geometry for the molecule that correlates to its ground state energy.

2.2. Optimization

Optimisations come after relaxation, in order to find the lattice vectors for crystal structure. Since $\text{CH}_3\text{NH}_3\text{PbBr}_3$ is a cubic structure, it holds that $\text{CH}_3\text{NH}_3\text{BiBr}_3$ and $\text{CH}_3\text{NH}_3\text{GaBr}_3$ should both be Cubic structures. As a result, only one lattice vector is required.

To optimise a molecular structure, a series of computations is carried out to find the total energy for a given set of lattice vectors in angstroms. The lattice vector that gives the lowest energy in electron-volts gives the most stable state. This was done using Linux supported shell scripts, and the total energy in electron-volts (eV) for each computation was plotted against the corresponding lattice vectors in angstroms (Å) using GRACE. FHI-aims' large scale eigen solver [8] (ELPA) was used for scalability and ELPA's efficient two-stage tridiagonalization [9] for accuracy.

3. Results and Discussion

3.1. Relaxation

Table 1 shows the relaxed geometries of $\text{CH}_3\text{NH}_3\text{BiBr}_3$ and $\text{CH}_3\text{NH}_3\text{GaBr}_3$ using trust radius algorithm, Tight atomic species, Perdew–Burke–Ernzerhof functional, and the Tkatchenko-Scheffler correction to consider van der Waals forces, as produced by FHI-aims [10].

These coordinates give the lowest total energy of the molecule considering the set parameters (trust radius algorithm, Tight atomic species, Perdew–Burke–Ernzerhof functional, and the Tkatchenko-Scheffler correction to consider van der Waals forces). This is the most stable geometry for the molecule that correlates to its ground state energy. These relaxed coordinates were used subsequently for optimization of lattice constants for $\text{CH}_3\text{NH}_3\text{BiBr}_3$ and $\text{CH}_3\text{NH}_3\text{GaBr}_3$ respectively.

3.2. Optimization

The plots (Fig. 1 and 2) are representations of the data resulting from the optimization of $\text{CH}_3\text{NH}_3\text{BiBr}_3$ and $\text{CH}_3\text{NH}_3\text{GaBr}_3$ for Total energy (eV) against Lattice vector (Å) for $\text{CH}_3\text{NH}_3\text{BiBr}_3$ and $\text{CH}_3\text{NH}_3\text{GaBr}_3$.

The optimisation and relaxation procedures are the first steps to establishing the proper basis for accurate band structure calculations and subsequently, optical properties. With this stage successfully passed, band structure calculations can be done using the optimized values for the lattice vectors for $\text{CH}_3\text{NH}_3\text{BiBr}_3$ and $\text{CH}_3\text{NH}_3\text{GaBr}_3$ which were found to be 9.10 Å and 8.27 Å respectively.

3.3. Visualization

The molecular and crystal structures of $\text{CH}_3\text{NH}_3\text{BiBr}_3$ and $\text{CH}_3\text{NH}_3\text{GaBr}_3$ of these perovskites were rendered using JMOL to interpret data provided by FHI-aims for their molecular geometry relaxation and lattice vector optimizations as shown by Table 1. Van der Waals forces were considered in a separate rendering to show the field carried by these compounds.

3.4. Density of States and Band Structure Calculations

The results gotten from the geometry relaxation and the lattice constant optimization were used as the fundamental conditioning criteria for the Band Structure and Density of States (DOS) calculations for $\text{CH}_3\text{NH}_3\text{BiBr}_3$ and $\text{CH}_3\text{NH}_3\text{GaBr}_3$ using FHI-aims code. Since perovskites are naturally cubic ($\text{CH}_3\text{NH}_3\text{PbBr}_3$ is cubic in nature), $\text{CH}_3\text{NH}_3\text{BiBr}_3$ and $\text{CH}_3\text{NH}_3\text{GaBr}_3$ should also be cubic assuming they are perovskites. A simple check to see if they are naturally Body-Centred Cubic (BCC) or Face-Centred Cubic (FCC) structures was done by running energy calculations of the two aforementioned structures. The structure with the lower calculated total energy in eV is the more stable structure and should be the natural state of the compounds.

Table 1. Relaxed Geometries

Compound	Relaxed Geometry (Using TRM) [x y z]	
CH ₃ NH ₃ BiBr ₃	atom 0.59330840, -1.08516916, -0.44146860	C
	atom 2.12315482, -1.69055848, 0.85207339	H
	atom 0.16764941, 0.56277636, -2.95052941	H
	atom 1.57739540, -0.12753172, 1.15036980	H
	atom 1.27679958, -1.10971028, 0.88647502	N
	atom -0.35410780, 0.98395270, -3.29044631	H
	atom 0.65850907, -1.43246174, 1.67565283	H
	atom 0.29085376, 2.09982157, 1.17408405	H
	atom -1.55998307, -0.68773874, -0.21933162	Bi
	atom 1.71597074, 2.07075197, 1.70759230	Br
	atom -1.65384372, -1.61237939, 2.31662933	Br
	atom -1.63570657, 2.02824692, 0.43889917	Br
CH ₃ NH ₃ GaBr ₃	atom 0.85461819, -0.64407212, -0.34519049	C
	atom 1.59617990, -2.53040013, 0.25626853	H
	atom 0.29015791, 0.47422585, -2.81100811	H
	atom 2.24221876, -1.28226252, 1.11699690	H
	atom 1.36344383, -1.64565233, 0.72336451	N
	atom -0.13852522, 0.86491294, -3.29034200	H
	atom 0.70278822, -1.83798565, 1.52272608	H
	atom -0.30945479, 2.92539614, 1.21890548	H
	atom -0.76367134, 0.08058922, 0.49274149	Ga
	atom 0.94130333, 2.95959971, 1.95201712	Br
	atom -1.33425958, -1.15115091, 2.50699603	Br
	atom -2.24479920, 1.78679980, -0.04347557	Br

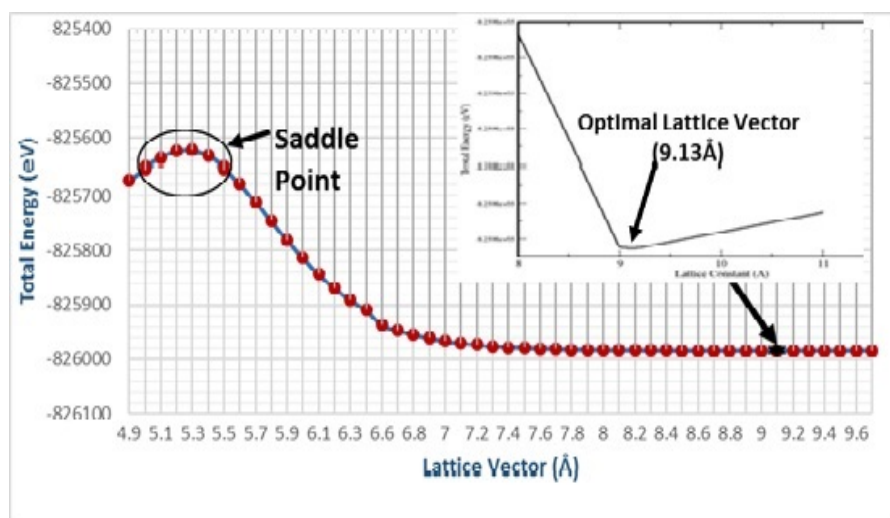


Figure 1. Total Energy (eV) vs Lattice Vector(Å) for CH₃NH₃BiBr₃ insert, showing the cropped plot section for the optimal lattice vector.

Afterwards, band structure calculations were implemented using fairly high convergent criteria; $12 \times 12 \times 12$ K-grid and $9 \times 9 \times 9$ DOS K-grid and the default suggestions for Light Atomic Species (using high convergence criteria, “Tight” or “Really Tight” for atomic species was not done because it was too computationally expensive for

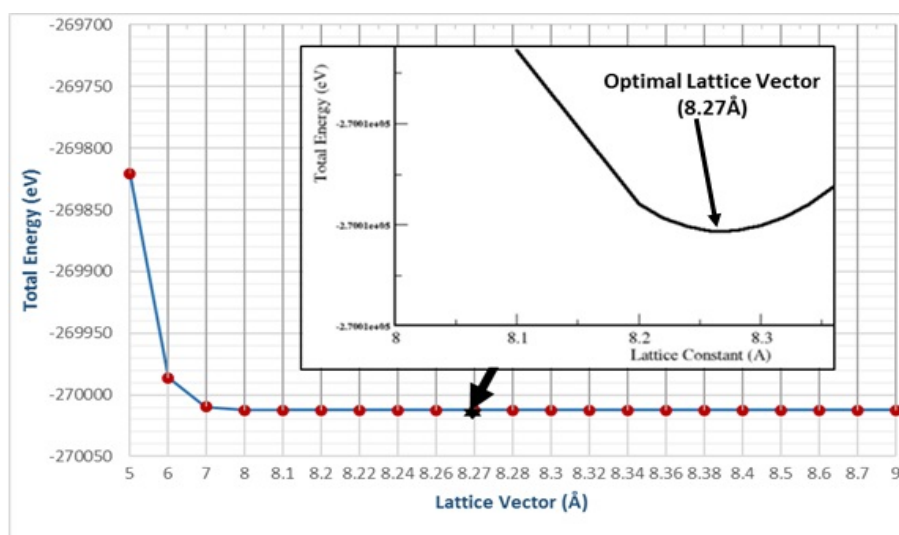


Figure 2. Total Energy (eV) vs Lattice Vector(Å) for $\text{CH}_3\text{NH}_3\text{GaBr}_3$ insert, showing the cropped plot section for the optimal lattice vector.

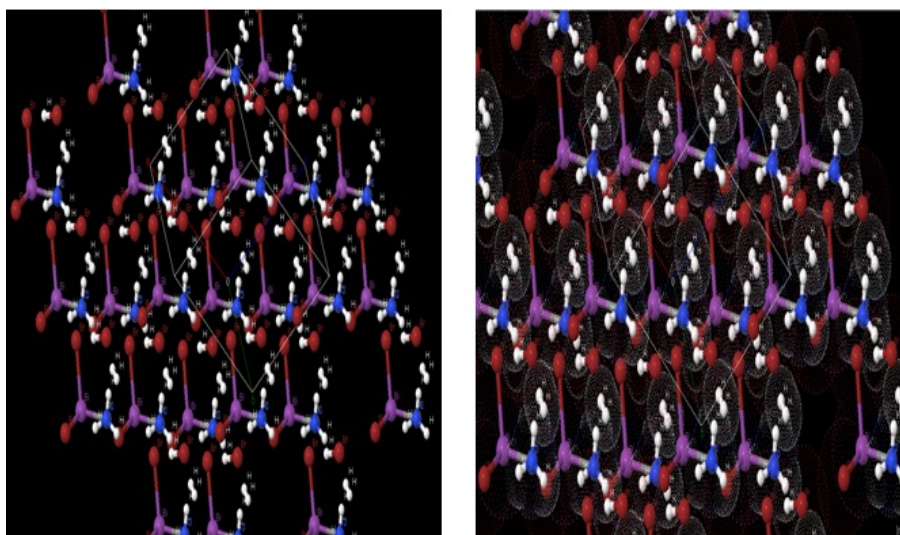


Figure 3. (a): JMOL Render of $\text{CH}_3\text{NH}_3\text{BiBr}_3$ BCC crystal structure (b): JMOL Render of $\text{CH}_3\text{NH}_3\text{BiBr}_3$ BCC crystal structure showing dot representation of van der Waals forces.

the computer hardware components used). The choice of lattice vectors implemented in FHI-aims is given in Table 2.

The corresponding band structure was calculated for symmetry k-points L, Γ , X, W and K which correspond to the points required for band structure plots for cubic systems. Included in the FHI-aims control.in file, the section of code in Fig. 7 shows the implementation for the band Structure and DOS calculation for the output of band data corresponding to the symmetry k-points mentioned above.

The Lowest Unoccupied Molecular Orbital (LUMO), Highest Occupied Molecular Orbital (HOMO) and calculated band gap is tabulated in Table 3. Band Structure and DOS plots were done to analyse the band structures of these crystals to see if they are Insulators (insulators have really high band gap in eV the Fermi level), Semiconductors (semiconductors have a relatively small band gap at the Fermi level as compared with insulators), or Metallic (have little or no band gap at the Fermi level). The Band structure and DOS plots resulting from the band structure

Figure 4. JMOL Render of $\text{CH}_3\text{NH}_3\text{BiBr}_3$ BCC crystal structure showing localized molecular

Table 2. BCC Lattice Structure Implementation

Conventional Lattice	Primitive Lattice	Implemented by FHI-aims	Remarks
$a_1 = (a, 0, 0)$	$a_1 = (-a/2, a/2, a/2)$	lattice vector $-a/2 \ a/2 \ a/2$	FHI-aims implements the primitive lattice as reproduced using the “lattice vector” keyword inputted in the geometry.in file before or after the specified atomic coordinates.
$a_2 = (0, a, 0)$	$a_2 = (a/2, -a/2, a/2)$	lattice vector $a/2 \ -a/2 \ a/2$	
$a_3 = (0, 0, a)$	$a_3 = (a/2, a/2, -a/2)$	lattice vector $a/2 \ a/2 \ -a/2$	

Where a is the lattice vector for cubic systems as $a=b=c$.

calculations are as shown in Figure 7 (a) and Figure 7 (b).

The resulting plots show that there are bands at the fermi level for both $\text{CH}_3\text{NH}_3\text{BiBr}_3$ and $\text{CH}_3\text{NH}_3\text{GaBr}_3$ thus there is a very small band gap suggesting that these materials are both metallic and are not fit for use as photoconductive materials in the fabrication of DSSCs. Bismuth and Gallium may be good substitutes for Lead in other materials but this study shows that they are not good replacements for Lead in the MAPbX_3 perovskite crystal structure. Table 3 shows the calculated LUMO, HOMO, and Band gap in eV, and the suggested material type based on the band gaps.

Still under debate are the theoretical optoelectronic properties of structures having the similar physical properties with MAPbX_3 because calculated band structure plots and diagrams are not similar, and are dependent on the level of approximation used; Figure 7 shows that MABiBr_3 and MAGaBr_3 are metallic in nature considering the Gaussian broadening method and the convergent criteria used (PBE_vdw). Obtaining a band gap that shows considerable concord with experimental findings does not mean that the band dispersion is significant [11].

This research was done using a compiled binary of the “scalapack.mpi” version of Fritz Haber Institute ab initio molecular simulation (FHI-aims) code (FHI-aims 171221.1 release) on the ELSI Electronic Structure Infrastructure [12] and ELPA library [8] to calculate the energies for the structural optimization of MABiBr_3 and MAGaBr_3 molecules, using additional software like GRACE (Graphing Advanced Computation and Exploration of data) and JMOL (Java Molecule) to graphically represent data and visualise the molecular structure(s) respectively. Regarding computer specifications, the computer used for this calculation was a Dell Inspiron N5110 notebook PC that has a quad-core Intel(R) Core (TM) i5-2430M CPU clocking up to 2.79GHz, with 8Gb of RAM running on the Linux-based Ubuntu 16.04 LTS.

Table 3. Calculated LUMO, HOMO and Band Gap Energies

MATERIAL	LUMO (eV)	HOMO (eV)	Band gap (eV)	Material Type
$\text{CH}_3\text{NH}_3\text{BiBr}_3$	-4.98522978	-4.98541615	0.00018636	Metallic
$\text{CH}_3\text{NH}_3\text{GaBr}_3$	-5.07541462	-5.07563748	0.0002286	Metallic

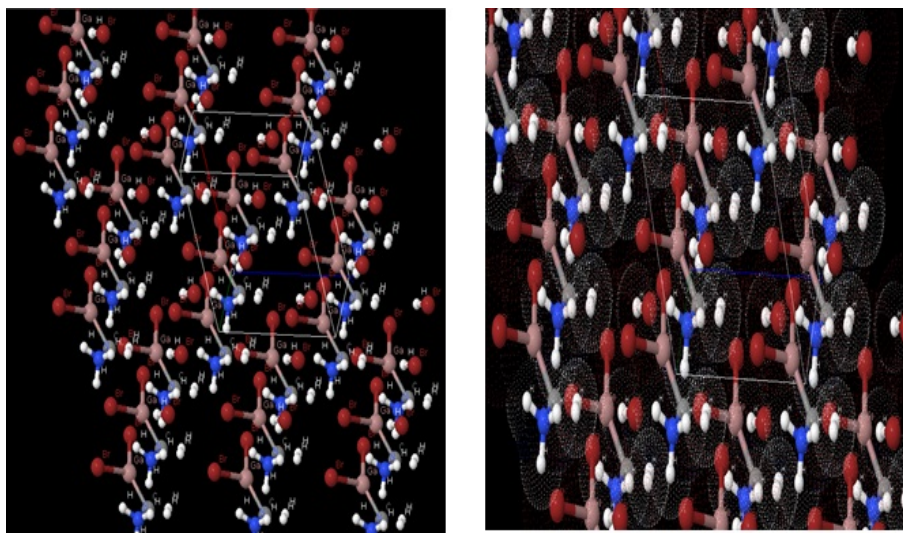


Figure 5. (a): JMOL Render of $\text{CH}_3\text{NH}_3\text{GaBr}_3$ BCC crystal structure (b): JMOL Render of $\text{CH}_3\text{NH}_3\text{GaBr}_3$ BCC crystal structure showing dot representation of van der Waals forces.

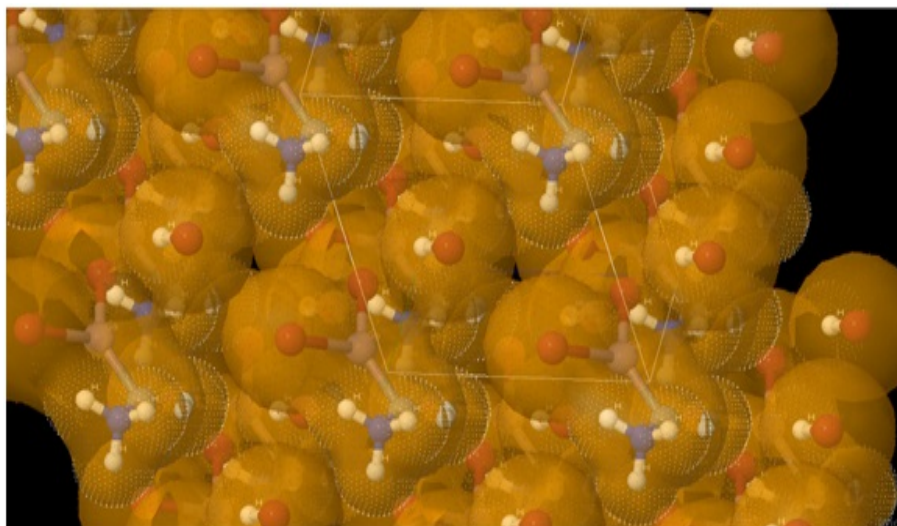


Figure 6. JMOL Render of $\text{CH}_3\text{NH}_3\text{GaBr}_3$ BCC crystal structure showing localized molecular packing structure with van der Waals forces.

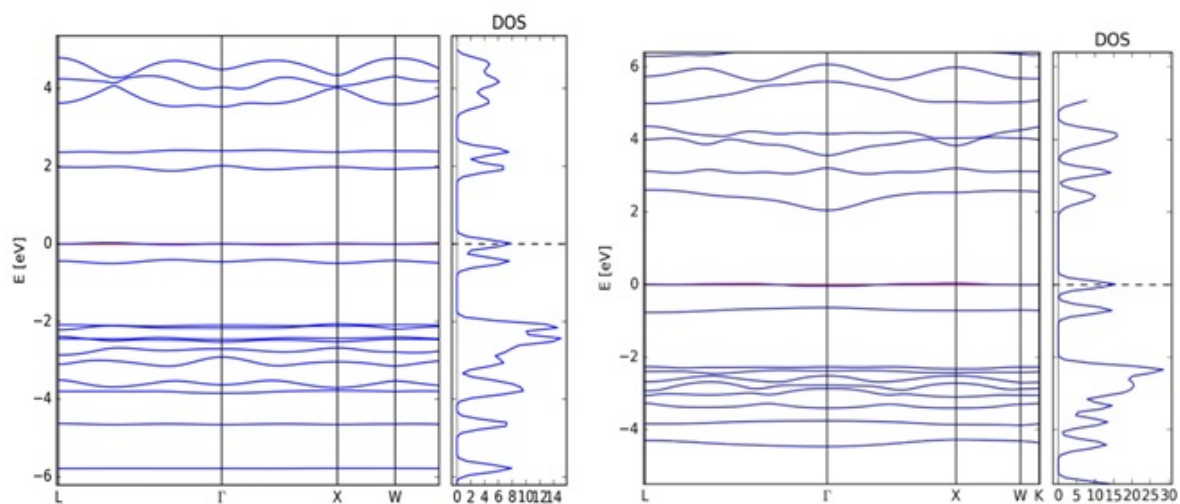


Figure 7. (a): Band structure and DOS plot for $\text{CH}_3\text{NH}_3\text{BiBr}_3$ with symmetry k-points L, Γ , X, W and K (b): Band Structure and DOS plot for $\text{CH}_3\text{NH}_3\text{GaBr}_3$ with symmetry k-points L, Γ , X, W and K.

4. Conclusion

In conclusion we have carried out the structural optimization, Band Structure analyses of $\text{CH}_3\text{NH}_3\text{BiBr}_3$ and $\text{CH}_3\text{NH}_3\text{GaBr}_3$ (having 8.33% dopant replacement percentage each) as possible replacements for the Lead based perovskite $\text{CH}_3\text{NH}_3\text{PbBr}_3$ using Perdew–Burke–Ernzerhof functional of Density Functional Theory as implemented by FHI-aims Code. Molecular visualizations and crystal structures were rendered using JMOL. Optimized lattice constants were calculated for $\text{CH}_3\text{NH}_3\text{BiBr}_3$ and $\text{CH}_3\text{NH}_3\text{GaBr}_3$ to be 9.10 Å and 8.27 Å respectively, and The Lowest Unoccupied Molecular Orbital (LUMO), Highest Occupied Molecular Orbital (HOMO) and calculated band gap, Band Structure and Density of States (DOS) plots were made to analyse the band structures of these crystals and they were found to be metallic with a band gap of 0.00018636 eV and 0.00022286 eV for $\text{CH}_3\text{NH}_3\text{BiBr}_3$ and $\text{CH}_3\text{NH}_3\text{GaBr}_3$ respectively.

References

- [1] L. Aurélien MA, P. Azarhoosh, M. I. Alonso, M. C. Oliver J. Weber, J. Yao & D. Bryant, “Experimental and Theoretical Optical Properties of Methylammonium Lead Halide Perovskites”, *Nanoscale* **8** (2016) 6317.
- [2] M. Carlo, F. El-Mellouhi, S. Kais, N. Tabet, F. Alharbi & S. Sanvito, “Revealing the Role of Organic Cations in Hybrid Halide Perovskite $\text{CH}_3\text{NH}_3\text{BiBr}_3$ ”, *Nature Communications* **6** (2015) 7026.
- [3] A. Hassan & G. Babaji, “First Principle Study on Lead-Free $\text{CH}_3\text{NH}_3\text{GeI}_3$ and $\text{CH}_3\text{NH}_3\text{GeBr}_3$ Perovskite Using FHI-aims Code”, *J. for Foundations and Applications of Physics* **6** (2019) 76.
- [4] H. Radhakrishna, “From Moore’s Law to Intel Innovation—prediction to Reality”, *Technolgy* **1** (2005).
- [5] Q. Claudio, E. Mosconi, J. M. Ball, V. D’Innocenzo, C. Tao, S. Pathak, H. J. Snaith, A. Petrozza & F. De Angelis, “Structural and Optical Properties of Methylammonium Lead Iodide across the Tetragonal to Cubic Phase Transition: Implications for Perovskite Solar Cells”, *Energy & Environmental Science* **9** (2016) 155.
- [6] D. Jianxu, Y. Zhao, S. Du, Yingshuang Sun, H. Cui, X. Zhan, X. Cheng & L. Jing, “Controlled Growth of MAPbBr_3 Single Crystal: Understanding the Growth Morphologies of Vicinal Hillocks on (100) Facet to Form Perfect Cubes” *J. M. science* **52** (2017) 7907.
- [7] A. C. Robert, C. Wolfram, K. P. De Jong, R. Gross, N. S. Lewis, B. Boardman, A. J. Ragauskas, K. Ehrhardt-Martinez, G. Crabtree & M. V. Ramana, “The Frontiers of Energy”, *Nature Energy* **1** (2016) 15020.
- [8] J. L. Simon, “Perovskites at the Nanoscale: From Fundamentals to Applications”, *Nanoscale* **8** (2017) 6206.
- [9] B. K. Andrew, “China’s Search for Renewable Energy: Pragmatic Techno-nationalism”, *Asian Survey* **53** (2013) 909.
- [10] P. Lyn, “Lead Toxicity, A Review of the Literature. Part I: Exposure, Evaluation, and Treatment”, *Alternative Medicine Review* **11** (2006).
- [11] S. Jayant, O. Lucon, A. Rahman, J. Christensen, F. Denton, J. Fujino & G. Heath, “Renewable Energy in the Context of Sustainable Development” (2011).
- [12] J. Dianxing, Y. Dang, Z. Zhu, H. Liu, C. Chueh, X. Li, L. Wang, X. Hu, A. K-Y. Jen & X. Tao, “Tunable Band Gap and Long Carrier Recombination Lifetime of Stable Mixed $\text{CH}_3\text{NH}_3\text{Pb}_x\text{Sn}_{1-x}\text{Br}_3$ Single Crystals”, *C. Materials* **30** (2018) 1556.